Synthesis, spectroscopic, and thermal investigation of transition and non-transition complexes of metformin as potential insulin-mimetic agents

Foziah A. Al-Saif · Moamen S. Refat

Abstract Complexes of $[Mn(MF)_2(Cl)_2]\cdot2H_2O$ (**1**), $[Fe(MF)_2(Cl)_2]Cl\cdot4H_2O$ (**2**), $[Ni(MF\cdot HCl)_2(Cl)_2]\cdot6H_2O$ (**3**), $[Cu(MF\cdot HCl)_2(Cl)_2]$ (**4**), $[Zn(MF\cdot HCl)_2](NO_3)_2\cdot6H_2O$ (**5**), $[Cd_2(MF\cdot HCl)(Cl)_4(H_2O)]$ (**6**), $[Mg(MF\cdot HCl)_2(Cl)_2]\cdot6H_2O$ (**7**), $[Sr_2(MF\cdot HCl)(Cl)_4(H_2O)]$ (**8**), $[Ba(MF\cdot HCl)_2(Cl)_2]\cdot2H_2O$ (**9**), $[Pt(MF)_4]$ (**10**), $[Au(MF)_3]Cl_3$ (**11**), and $[Pd(MF)_2]Cl_2$ (**12**) were synthesized from Legitional behavior of metformin drug as a diabetic agent. The authenticity of the transition and non-transition metal complexes were characterized by elemental analyses, molar conductivity, (infrared, UV–Vis) spectra, effective magnetic moment in Bohr magnetons, electron spin resonance, thermal analysis, X-ray powder diffraction as well as scanning electron microscopy. Infrared spectral studies as well as elemental analyses revealed the existence of metformin in the base or hydrochloride salt forms in the chelation state acts as a bidentate ligand while the platinum(IV) complex is coordinated through the deprotonation of –NH group. The magnetic and electronic spectra of Mn(II), Fe(III), Ni(II), and Cu(II) complexes suggest an octahedral geometry. Antimicrobial screening of metformin and its complexes were determined against the (G^+ and G^-) bacteria (*Escherichia coli*, *Staphylococcus aureus*, *Bacillus subtilis*, and *Pseudomonas aeruginosa*) and fungi (*Aspergillus flavus* and *Candida albicans*).

Keywords Metformin · Transition and non-transition metals · Thermal studies · Spectroscopic investigation · Antimicrobial test

F. A. Al-Saif
Department of Chemistry, Faculty of Science,
Princess Nora Bint Abdul Rahman University,
Riyadh, Kingdom of Saudi Arabia

M. S. Refat (✉)
Department of Chemistry, Faculty of Science,
Port Said University, Port Said, Egypt
e-mail: msrefat@yahoo.com

M. S. Refat
Department of Chemistry, Faculty of Science,
Taif University, 888, Taif, Kingdom of Saudi Arabia

Introduction

Metformin hydrochloride (MF·HCl) (Fig. 1), (*N,N*-dimethyl-imido-dicarbonimidic diamide hydrochloride) or 1,1-dimethylbiguanide, it has two imino (–C=NH) and one each of primary (–NH_2), secondary (–NH), tertiary (–N(CH_3)_2) amino groups as donating centers. Metformin is commonly prescribed agent for the treatment of type II diabetes, induces multiple beneficial effects including weight loss and lipid reduction in addition to lowering blood glucose levels [1, 2]. It is an oral hypoglycemic agent, which enhances insulin sensitivity and is not effective in the absence of insulin [3]. It lowers blood glucose level in NIDDM patients by suppressing hepatic glucose output and enhancing peripheral glucose uptake. The mechanism of action involves binding of the polar biguanide hydrocarbon side-chain to membrane phospholipids, evoking a change in the electrostatic surface potential [4]. Subsequently, various metabolic effects are elicited, depending on the target cell, tissue, organ, species [5, 6], and metabolic regulation [7]. The available data on the relationship of structure to hypoglycemic activity for metformin has extensively been studied [8, 9]. Metformin is incompletely absorbed, facile recovery being about 30 % of an oral dose [10], the absorption is slower than the

elimination. Oral bioavailability was 50–60 % of the dose [11]. The difference between absorbed and available drug may reflect minor presynaptic clearance of the drug [10] or binding to the intestinal wall [12]. Concomitant food intake may slightly impair metformin absorption [13]. Metformin, because of its chemical structure, does not interact with the liver and has a short half-life [14]. Higher doses may be associated with an increased incidence of gastrointestinal adverse effects [15]. Metformin combines with many elements of the transition series, especially copper(II), nickel(II), cobalt(II), and platinum(II) as [PtCl(MF)(DMSO)]Cl, [PtCl$_4$(MF)(DMSO)], [Co(MF·HCl)(Cl)$_2$], [CuCl$_2$(MF)$_2$], [Cu(MF)$_2$]Cl$_2$·2H$_2$O, [Ni(MF)$_2$](Cl)(OH), and [Zn(MF·HCl) Cl$_2$] [16–19]. The metal complexes of metformin ligand are usually cationic in nature, and their highly color chelate varies with the nature of the metal ion and its oxidation state, as well as with the number of ligands in the complex due to the presence of the two imine groups in *cis* position thus acting as a chelating agent.

Metal complexes preparation has been the focus because of enhanced biological activities of the corresponding drug metal complexes [16]. New Little attention for antimicrobial activities evaluations have been previously reported in the literature for metformin metal complexes. This paper is a continuation of our research [20–23] in the field of chelation between the transition and non-transition metal salts with dynamic pharmaceutical compounds, which are commonly used. The goal of this research is mainly to synthesize Mn(II), Fe(III), Ni(II), Cu(II), Zn(II), Pd(II), Cd(II), Pt(IV), Au(III), Mg(II), Ba(II), and Sr(II) have been characterized elemental analyses, molar conductivity, (infrared, UV–Vis) spectra, effective magnetic moment in Bohr magnetons, electron spin resonance (ESR), thermal analysis (TG), X-ray powder diffraction (XRD) as well as scanning electron microscopy (SEM). In addition, the in vitro antimicrobial and antitumor activities were assessment against some kind of (G$^+$ and G$^-$) bacteria and fungi (*Escherichia coli*, *Staphylococcus aureus*, *Bacillus subtilis* and *Pseudomonas aeruginosa*) and (*Aspergillus flavus* and *Candida albicans*), respectively, were reported. This article

adds to the studies regarding to obtain the new complexes of metformin with potential insulin-mimetic agents.

Experimental

Chemicals

All chemicals were bought and used without further purification. Metformin HCl (MF·HCl), transition and non-transition metal salts (manganese(II) chloride tetrahydrate, ferric(III) chloride hexahydrate, nickel(II) chloride hexahydrate, copper(II) chloride dihydrate, zinc(II) nitrate hexahydrate, palladium(II) chloride, cadmium(II) chloride monohydrate, platinum(IV) chloride (H$_2$PtCl$_6$), sodium gold(III) hydrate, magnesium(II) chloride hexahydrate, strontium(II) chloride hydrate, and barium(II) chloride dihydrate) were received from BDH and Aldrich Companies, and other chemicals and solvents used as it is without purification.

Synthesis of MF·HCl complexes

An aqueous solutions 30 mL distilled water of metformin hydrochloride, MF·HCl, ligand (2.0 mmol; 0.332 g) and 20 mL (1.0 mmol) of an aqueous solutions of MnCl$_2$·4H$_2$O (0.198 g), NiCl$_2$·6H$_2$O (0.192 g), CuCl$_2$·2H$_2$O (0.170 g), Zn(NO$_3$)$_2$·6H$_2$O (0.297 g), PdCl$_2$ (0.177 g), CdCl$_2$·H$_2$O (0.201 g), PtCl$_4$ as (H$_2$PtCl$_6$) (0.410 g), MgCl$_2$·6H$_2$O (0.204 g), SrCl$_2$·H$_2$O (0.177 g) or BaCl$_2$·2H$_2$O (0.263 g) were mixed with refluxed at 70 °C for 45 min. The colored solid precipitated which separated on cooling were filtered, washed several times with water and little amount of methanol. Concerning complexes of FeCl$_3$·6H$_2$O (0.270 g), or NaAuCl$_4$·H$_2$O (0.40 g), the reaction mixture occurs as the same procedure, but with molar ratio 1:3 (metal:MF· HCl). It should be noted that, the Mn(II), Fe(III), Pt(IV), Au(III), and Pd(II) metformin complexes were precipitated with gradually addition of 0.1 M aqueous NH$_4$OH solution.

Fig. 1 Structure of metformin (MF) ligand
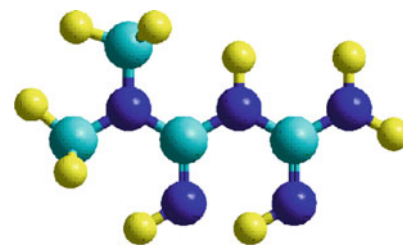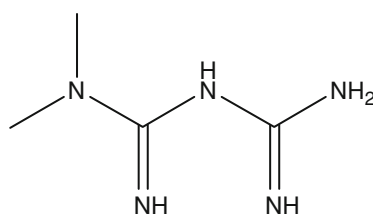
The resulting metformin hydrochloride complexes were dried under vacuum over anhydrous calcium chloride.

Measurements

The elemental analyses of carbon, hydrogen, and nitrogen contents were performed by the microanalysis unit at Cairo University, Egypt, using a Perkin Elmer CHN 2400 (USA). The percentage of respective metals in the solid reaction products were determined gravimetrically by transforming the products into oxides. The molar conductivities of freshly prepared 1.0×10^{-3} mol/cm^3 dimethylsulfoxide (DMSO) solutions were measured for the dissolved MF·HCl complexes using Jenway 4010 conductivity meter. The electronic absorption spectra of MF·HCl complexes were recorded in DMSO solvent within 900–200 nm range using a UV2 Unicam UV/Vis Spectrophotometer fitted with a quartz cell of 1.0 cm path length in Mansoura University. The infrared spectra with KBr discs were recorded on a Bruker FT-IR Spectrophotometer (4,000–400 cm^{-1}). Solid reflectance spectra were measured on UV-3101 PC, Shimadzu, UV–Vis NIR Scanning Spectrophotometer. Magnetic data were calculated using Magnetic Susceptibility Balance, Sherwood Scientific, Cambridge Science Park Cambridge, England, at temp 25 °C in Cairo University. The ^{1}H-NMR spectra were recorded on Varian Mercury VX-300 NMR spectrometer. ^{1}H spectra were run at 300 MHz spectra in deuterated dimethylsulfoxide (DMSO-d$_6$). Chemical shifts are quoted in δ and were related to that of the solvents. The ESR spectrum for copper(II)/MF·HCl complex was performed on Jeol, JES-FE2XG, ESR-spectrometer, Frequency 9.44 GHz with Jeol Microwave unit. The thermal studies TG/DTG-50H were carried out on a Shimadzu thermogravimetric analyzer under static air till 800 °C. SEM images were taken in Quanta FEG 250 equipment. The X-ray diffraction patterns for the selected metformin HCl complexes were recorded on X 'Pert PRO PANanalytical XRD, target copper with secondary monochromate.

Antibacterial and antifungal activities

Antimicrobial activity of the tested samples was determined using a modified Kirby–Bauer disc diffusion method [24]. In brief, 100 µL of the best bacteria/fungi were grown in 10 mL of fresh media until they reached a count of approximately 108 cells/mL for bacteria or 105 cells/mL for fungi [25]. 100 µL of microbial suspension was spread onto agar plates corresponding to the broth in which they were maintained. Isolated colonies of each organism that might be playing a pathogenic role should be selected from primary agar plates and tested for susceptibility by disk diffusion method [26, 27]. Of the many media available, National Committee for Clinical Laboratory Standards (NCCLS) recommends Mueller-Hinton agar due to: it results in good batch-to-batch reproducibility. Disk diffusion method for filamentous fungi tested by using approved standard method (M38-A) developed by the NCCLS [28] for evaluating the susceptibility of filamentous fungi to antifungal agents. Disk diffusion method for yeast developed standard method (M44-P) by the NCCLS [29]. Plates inoculated with filamentous fungi as *A. flavus* at 25 °C for 48 h; Gram (+) bacteria as *S. aureus*, *B. subtilis*; Gram (−) bacteria as *E. coli*, *P. aeruginosa* they were incubated at 35–37 °C for 24–48 h and yeast as *C. albicans* incubated at 30 °C for 24–48 h and, then the diameters of the inhabitation zones were measured in millimeters [24]. Standard disks of tetracycline (antibacterial agent), amphotericin B (antifungal agent) served as positive controls for antimicrobial activity but filter disk impregnated with 10 µL of solvent (distilled water, DMSO) were used as a negative control. Blank paper disks (Schleicher & Schuell, Spain) with a diameter of 8.0 mm were impregnated 10 µL of tested concentration of the stock solutions. Agar-based methods such as Etest disk diffusion can be good alternatives because they are simpler and faster than broth methods [30, 31].

Results and discussion

In the present study, metal complexes of metformin hydrochloride were prepared using Mn(II), Fe(III), Ni(II), Cu(II), Zn(II), Cd(II), Mg(II), Sr(II), Ba(II), Pt(IV), Au(III) and Pd(II), the resulting complexes were discussed and created to serve as potential insulin-mimetic. The physical appearance and analytical data of the twelve transitions and non-transition complexes were summarized in Table 1. The elemental analysis shows that Mn(II), Fe(III), Ni(II), Cu(II), Zn(II), Mg(II), Ba(II), and Pd(II) formed complexes with metformin in 1:2 (metal:MF) ratio, while (Cd(II) and Sr(II)), Au(III) and Pt(IV) formed with molar ratios (metal:MF) 2:1, 1:3 and 1:4, respectively. All synthesized complexes are colored and possess high melting points. The complexes are partially soluble in hot methanol and insoluble in water and some other organic solvents except for DMSO and dimethylformamide. Without X-ray analysis, no definite formula structures can be suggested. However, spectroscopic (infrared, UV–Vis and ESR), effective magnetic moment and elemental analyses data led us to suggest structures. The colors, conductivity, elemental analysis data and compositions of the MF complexes are given in Table 1.

Table 1 Analytical and physical data for metformin HCl and their metal complexes

Complexes Empirical formula/mol. wt./(g/mol)	Color	$\Lambda m/\Omega^{-1}$ cm^{-1} mol^{-1}	Elemental analysis/% found/calcd.			
			C	H	N	M
[Mn(MF)$_2$(Cl)$_2$]·2H$_2$O (**1**) (420.17)	Brown	54	23.15/22.85	5.84/5.24	32.55/33.32	12.87/13.08
[Fe(MF)$_2$(Cl)$_2$]Cl·4H$_2$O (**2**) (492.53)	Brown	72	19.39/19.49	6.44/6.09	28.04/28.43	11.21/11.34
[Ni(MF·HCl)$_2$(Cl)$_2$]·6H$_2$O (**3**) (569.02)	Green	62	17.16/16.87	6.24/6.33	24.00/24.60	10.12/10.32
[Cu(MF·HCl)$_2$(Cl)$_2$] (**4**) (465.71)	Turquoise	55	20.61/20.61	5.08/5.15	29.81/30.06	13.44/13.65
[Zn(MF·HCl)$_2$](NO$_3$)$_2$·6H$_2$O (**5**) (628.75)	White	81	15.80/15.27	5.04/5.73	27.32/26.72	10.25/10.40
[Cd$_2$(MF·HCl)(Cl)$_4$(H$_2$O)] (**6**) (550.27)	White	56	7.63/8.72	2.46/2.54	12.00/12.72	39.96/40.86
[Mg(MF·HCl)$_2$(Cl)$_2$]·6H$_2$O (**7**) (534.57)	White	49	18.16/17.96	8.26/6.73	25.93/26.19	4.22/4.55
[Sr$_2$(MF·HCl)(Cl)$_4$(H$_2$O)] (**8**) (500.69)	White	51	10.37/9.59	2.56/2.79	13.02/13.98	34.27/35.00
[Ba(MF·HCl)$_2$(Cl)$_2$]·2H$_2$O (**9**) (575.52)	White	48	16.13/16.68	5.03/4.86	24.78/24.33	23.36/23.86
[Pt(MF)$_4$] (**10**) (711.55)	Yellow	20	26.26/26.98	6.61/5.62	39.73/39.35	27.23/27.42
[Au(MF)$_3$]Cl$_3$ (**11**) (690.82)	Orange	110	20.64/20.84	4.61/4.78	31.43/30.40	28.25/28.51
[Pd(MF)$_2$]Cl$_2$ (**12**) (435.66)	Brown	87	22.00/22.04	4.97/5.05	32.02/32.13	24.30/24.42

Molar conductance

The conductivity of metformin complexes was measured in DMSO solvent at room temperature. All the complexes showed the molar conductance values for 10^{-3} mol/cm^3 concentration in range of 20–110 ohm^{-1} cm^2 mol^{-1}. It is suggesting that metformin complexes have three types of conductance nature [32, 33], (i) electrolyte nature for Fe(III), Zn(II), Au(III), and Pd(II) complexes according to the location of chloride ion outside the coordination sphere, (ii) slightly electrolyte nature for Mn(II), Ni(II), Cu(II), Cd(II), Mg(II), Sr(II), and Ba(II) complexes due to the sharing of anion (chloride or nitrate ion) in the chelation process, also, the difference in the values of molar conductance between these complexes is due to the presence of metformin in salt form (metformin HCl), and (iii) non electrolyte nature for Pt(IV) complex which has a low conductance values ~ 20 ohm^{-1} cm^2 mol^{-1} comparing with the initial components. The molar conductance values of the resulted complexes are listed in Table 1. The presence of chloride ions or hydrochloric molecule in all metformin complexes except for zinc(II) and platinum(IV) complexes was detected by the addition of few drops of concentrated silver nitrate reagent leading to the appearance of white precipitate.

Infrared spectra

The discussion of infrared absorption bands are one of the important tool of analyses used for determining the mode of chelations. The most significant bands (Table 2) of metformin HCl ligand can be classified into three sections (i) NH vibrational spectra of primary (–NH$_2$), secondary (–NH) and imino (–C=NH) groups, (ii) C–N and C=N vibrational bands, and (iii) C–H vibrations of the two

methyl groups. According, the above three fundamental vibrational sections, the metformin HCl free ligand can be interpretative as follows; N–H Vibrations: (i) The N–H stretching of C=N–H group occurs in the region 3,400–3,100 cm^{-1}. Usually the frequency of this vibration is decreased in the presence of hydrogen bond [34]. The broadening bands at 3370 cm^{-1} and 3294, 3174 cm^{-1} has been assigned to N–H asymmetric and symmetric stretching vibrations, respectively. The band at 1,570 cm^{-1} has been assigned for NH$_2$ in plane deformation vibrations [35]. The bands of medium-to-weak intensity at 935, 798, and 735 cm^{-1} are due to N–H wagging. (ii) C=N, C–N vibrations: Metformin HCl has strong absorption band at 1,627 cm^{-1} which is due to C=N stretching vibration [35]. The medium-to-weak intensity bands in the FTIR spectra at 1271, 1168, and 1061 cm^{-1} have been assigned to C–N stretching vibrations of aliphatic amine compounds. Medium-to-weak intensity bands at 639, 582, 541, and 419 cm^{-1} are due to CNC deformation vibrations [35]. C–H Vibrations: CH stretching vibration (asymmetric and symmetric) of the aliphatic methyl group which existed at 2,975–2,950 cm^{-1} for the asymmetric and at 2,885–2,865 cm^{-1} for symmetric CH$_3$ stretching vibrations [36]. In metformin HCl, the presence of nitrogen near methyl group reduces the symmetric CH$_3$ stretching range as 2,835–2,815 cm^{-1} [37, 38]. Bands at 2965, 2920, and 2813 cm^{-1} are assigned to CH asymmetric and symmetric stretching vibrations of the methyl group. The methyl group has a three deformation bands with medium intensity at 1479, 1448, and 1417 cm^{-1} [35].

The presence of infrared spectral bands attributed to the imino groups (–C=NH), at the same places of metformin HCl free ligand with significant intensity shift in the complex formation, which indicates that metformin is coordinated toward metal ions through nitrogen atom of

Table 2 Assignments of the infrared spectral bands (cm^{-1}) for metformin HCl and their metal complexes

Compound	Assignments								
	v_{as} (NH)	v_s (NH)	v (CH$_3$)	v (C=N)	δ_{def} (NH$_2$)	δ (CH$_3$)	v (C–N)	δ_w (NH)	δ_{def} (CNC) v (M–N)
MF·HCl	3,370	3,174	2,965	1,627	1,570	1,479	1,271	935	639
	3,294		2,920			1,448	1,168	798	582
			2,813			1,417	1,061	735	541
									419
[Mn(MF)$_2$(Cl)$_2$]·2H$_2$O (**1**)	3,370	3,173	2,960	1,628	1,570	1,479	1,270	936	639
	3,296		2,918			1,449	1,169	799	583
			2,813			1,417	1,062	735	543
									419
[Fe(MF)$_2$(Cl)$_2$]Cl·4H$_2$O (**2**)	3,370	3,164	3,000	1,685	1,582	1,485	1,265	935	660
	3,291			1,629		1,446	1,219	839	550
						1,404	1,170	799	512
							1,142	735	418
							1,059		
[Ni(MF·HCl)$_2$(Cl)$_2$]·6H$_2$O (**3**)	3,368	3,172	–	1,681	1,582	1,479	1,294	933	639
	3,292					1,449	1,271	893	608
						1,416	1,167	796	572
							1,060	734	538
									418
[Cu(MF·HCl)$_2$(Cl)$_2$] (**4**)	3,356	3,182	3,098	1,663	1,547	1,501	1,308	888	614
	3,286		3,013			1,450	1,223	774	559
						1,381	1,180	708	427
							1,142	674	414
							1,059		404
[Zn(MF·HCl)$_2$](NO$_3$)$_2$·6H$_2$O (**5**)	3,574	3,223	2,933	1,761	1,544	1,454	1,279	960	632
	3,421			1,657		1,383	1,242	935	523
	3,323			1,637			1,172	826	464
							1,143	721	
							1,106		
							1,053		
[Cd$_2$(MF·HCl)(Cl)$_4$(H$_2$O)] (**6**)	3,447	3,126	2,960	1,634	1,588	1,418	1,276	932	634
	3,408		2,882		1,532		1,255	716	605
	3,326		2,814				1,206		557
	3,230						1,145		506
							1,048		
[Mg(MF·HCl)$_2$(Cl)$_2$]·6H$_2$O (**7**)	3,371	3,175	–	1,628	1,582	1,479	1,167	933	638
						1,449	1,059	793	608
						1,418		733	573
									537
									421
[Sr$_2$(MF·HCl)(Cl)$_4$(H$_2$O)] (**8**)	3,370	3,174	2,813	1,629	1,569	1,478	1,271	936	700
	3,296					1,448	1,168	799	656
						1,416	1,062	734	581
									544
									420

Table 2 continued

Compound	Assignments								
	v_{as} (NH)	v_s (NH)	v (CH$_3$)	v (C=N)	δ_{def} (NH$_2$)	δ (CH$_3$)	v (C–N)	δ_w (NH)	δ_{def} (CNC)v (M–N)
[Ba(MF·HCl)$_2$(Cl)$_2$]·2H$_2$O (**9**)	3,455	3,174	2,813	1,628	1,576	1,480	1,271	935	661
	3,370					1,449	1,169	799	570
	3,324					1,418	1,062	734	544
	3,297					1,369			418
[Pt(MF)$_4$] (**10**)	3,371	3,164	2,813	1,629	1,570	1,478	1,272	935	698
	3,297					1,448	1,245	798	657
						1,415	1,208	736	583
							1,168		543
							1,062		419
[Au(MF)$_3$]Cl$_3$ (**11**)	3,370	3,169	–	1,629	1,568	1,476	1,271	934	651
	3,296					1,448	1,202	797	581
						1,409	1,167	735	539
							1,061		419
[Pd(MF)$_2$]Cl$_2$ (**12**)	3,145	3,044	2,807	1,747	1,508	1,402	1,206	894	702
				1,680			1,074	827	510
				1,642					450

v_s stretching symmetry; v_{as} stretching asymmetric; δ bending

imino group without proton displacement. The second assumption that, the stretching vibrational bands of v_{as}(NH) and v_s(NH) of (primary and secondary) amino group as well as imino group did not greatly affected by chelation, which show on the non-participation of both –NH$_2$ and –NH, in addition the non-displacement of imino group (–C=NH) in complexation process of metformin ligand. The third guide which denies the non displacement of imino group, is the presence of stretching vibration band of v(C=NH) at the same or shifted to higher frequencies position of metformin free ligand. In addition to this, the spectrum exhibit characteristic vibrational frequencies of ionic nitrate group of zinc(II) complex (**5**). A very strong band observed at about 1,383 cm^{-1} indicates the presence of ionic nitrate group [39]. In these complexes and it is due to the v_3 vibration of the nitrate group of D$_{3h}$ symmetry. This is supported by another band of medium intensity appeared at 826 cm^{-1}, which is attributed to the v_2 vibration of the ionic nitrate [39]. The infrared spectra of distinguish bands of water molecules concerning hydrated MF complexes were existed overlapping with characteristic bands of amino group.

Electronic spectra and magnetic measurements

Both Tables 3 and 4 refer to the electronic (UV–Vis and solid reflectance) spectra and magnetic measurements

assignments which are important and interesting items for most chemical characterizations to draw important information about the structural aspects of the complexes. Metformin hydrochloride free ligand, which is vital organic compound, has absorption in the ultraviolet (228, 262, and 284 nm) and visible (375 nm) regions in the region of the 200–900 nm and in some cases these bands extends over to higher wavelength region due to conjugation. But upon complexation with transition and non-transition metal ions, due to interaction with the metal ion there will be an interesting change in the electronic properties of the system. New bands in the visible region due to d–d absorption and charge transfer spectra from metal to ligand (M–L) or ligand to metal (L–M) can be observed and this data can be processed to obtain information regarding the structure and geometry of the complexes [40]. Electronic spectra of complexes were recorded in DMSO with 10^{-3} mol/cm^3. UV–Visible peaks corresponding to the $\pi \rightarrow \pi^*$ transitions in the MF complexes were observed at 230 and 264 nm for Mn(II)/MF complex (**1**), (272 and 296 nm) for Fe(III)/MF complex (**2**), 266 nm for Ni(II)/MF complex (**3**), 280 nm for Cu(II)/MF complex (**4**), (226 and 264 nm) for Zn(II)/MF complex (**5**), (258 and 288 nm) for Cd(II)/MF complex (**6**), (220, 240, and 258 nm) for Mg(II)/MF complex (**7**), (230 and 258 nm) for Sr(II)/MF complex (**8**), 250 nm for Ba(II)/MF complex (**9**), (250 and 268 nm) for Pt(IV)/MF complex (**10**), 282 nm for Au(III)/MF complex (**11**) and

Table 3 Electronic spectral bands (nm) and magnetic moments of the metformin HCl complexes

Complexes	λ/nm transitions			μ_{eff}/B.M.	n	Hybrid orbitals	Spin-only/B.M.	Stereo-chemistry
	$\pi \rightarrow \pi^*$	n $\rightarrow \pi^*$	LMCT					
MF·HCl	228	375	–	–	–	–	–	–
	262							
	284							
[Mn(MF)$_2$(Cl)$_2$]·2H$_2$O (**1**)	230	324	–	3.18	1	d^2sp^3	1.73	Octahedral
	264							
[Fe(MF)$_2$(Cl)$_2$]Cl·4H$_2$O (**2**)	272	320	406	2.00	1	d^2sp^3	1.73	Octahedral
	296	354	490					
		364						
[Ni(MF·HCl)$_2$(Cl)$_2$]·6H$_2$O (**3**)	266	328	406	0	0	d^2sp^3	0	Octahedral
		382	612					
			678					
			742					
[Cu(MF·HCl)$_2$(Cl)$_2$] (**4**)	280	310	434	1.23	1	sp^3d^2	1.73	Octahedral
			636					
[Zn(MF·HCl)$_2$](NO$_3$)$_2$·6H$_2$O (**5**)	226	308	–	–	–	–	–	Six coordinate
	264							
[Cd$_2$(MF·HCl)(Cl)$_4$(H$_2$O)] (**6**)	258	378	–	–	–	–	–	Four coordinate
	288							
[Mg(MF·HCl)$_2$(Cl)$_2$]·6H$_2$O (**7**)	220	–	–	–	–	–	–	Six coordinate
	240							
	258							
[Sr$_2$(MF·HCl)(Cl)$_4$(H$_2$O)] (**8**)	230	382	–	–	–	–	–	Four coordinate
	258							
	302							
[Ba(MF·HCl)$_2$(Cl)$_2$]·2H$_2$O (**9**)	250	–	–	–	–	–	–	Six coordinate
[Pt(MF)$_4$] (**10**)	250	372	–	–	–	–	–	Four coordinate
	268							
[Au(MF)$_3$]Cl$_3$ (**11**)	282	–	–	–	–	–	–	Six coordinate
[Pd(MF)$_2$]Cl$_2$ (**12**)	230	374	–	–	–	–	–	Four coordinate
	242							
	260							
	298							

n unpaired electrons

(230, 242 and 260 nm) for Pd(II)/MF complex (**12**) [41]. The peaks belonging to n $\rightarrow \pi^*$ transitions are recorded a wavelengths 375, 324 nm, (320, 354, and 364 nm), (328 and 382 nm), 310, 308, 378, 382, 372, and 374 nm, respectively, for MF·HCl, **1**, **2**, **3**, **4**, **5**, **6**, **8**, **10**, and **12** metformin HCl complexes [42]. The first range can be assigned to $\pi \rightarrow \pi^*$ transitions in the aromaticity of double bond while the second range is most probably due to the n $\rightarrow \pi^*$ transitions of imine (=NH), primary (–NH$_2$), secondary (–NH), and tertiary (–N(CH$_3$)$_2$) amino groups. The third type of transition in visible region located at (406 and 490 nm) for complex **2**, (406, 612, 678, and 742 nm) for complex **3**, and (434 and 636 nm) for complex **4**, can be

attributed to the ligand-to-metal charge transfer bands LMCT from the electronic lone pairs of respective nitrogen to the metal ions [43]. The electronic spectrum of the MF·HCl ligand exhibited maximum band at 375 nm, which could be assigned to the n–π^* transition of the imine (=NH), primary (–NH$_2$), and secondary (–NH) amino groups. This band show a blue shift or decreasing for the absorbance intensity in all MF·HCl complexes. This clearly indicates the coordination of the imine nitrogen atom with the metal atom. Furthermore, the detectable medium-to-strong intensity bands within the range of 220–300 nm due to π–π^* transitions in the free MF·HCl ligand were changed in the spectra of the metal complexes.

Table 4 Solid reflectance spectral bands (cm^{-1}) and assignments of the metformin HCl complexes

Complexes	Spectra data/cm^{-1}	Electronic transition	Assignments
[Mn(MF)$_2$(Cl)$_2$]·2H$_2$O (**1**)	16,529	$^6A_{1g} \rightarrow {}^4T_{1g}$(G)	Distorted octahedral
	17,731	$^6A_{1g} \rightarrow {}^4T_{2g}$(G)	
	19,531	$^6A_{1g} \rightarrow {}^4E_g$(G), $^4A_{1g}$(G)	
	20,747		
[Fe(MF)$_2$(Cl)$_2$]Cl·4H$_2$O (**2**)	16,129	$^6A_1 \rightarrow {}^4A_1$, ^4E(G)	Distorted octahedral
	21,097	$^6A_1 \rightarrow {}^4T_2$(G)	
[Ni(MF·HCl)$_2$(Cl)$_2$]·6H$_2$O (**3**)	14,749	$^3A_{2g}$(F) $\rightarrow {}^3T_{1g}$(F)	Distorted octahedral
	22,422	$^3A_{2g}$(F) $\rightarrow {}^3T_{1g}$(P)	
[Cu(MF·HCl)$_2$(Cl)$_2$] (**4**)	15,038	$^2B_{1g} \rightarrow {}^2E_g$	Distorted octahedral
	20,284	$^2B_{1g} \rightarrow {}^2B_{2g}$	

Magnetic susceptibility measurement in a magnetic field, the paramagnetic complexes will be attracted while the diamagnetic compounds repelled. The zinc(II), cadmium(II), magnesium(II), strontium(II), and barium(II) complexes are diamagnetic moments. In paramagnetic manganese(II), ferric(III), nickel(II), and copper(II) complexes, often the magnetic moment (μ_{eff}) gives the spin only value ($\mu_{s.o.} = (n(n + 2))^{1/2}$ B.M.) corresponding to the number of unpaired electron. The variation from the spin only value is attributed to the orbital contribution and it varies with the nature of coordination and consequent delocalization. A mononuclear complex of manganese(II) of the formula [Mn(MF)$_2$(Cl)$_2$]·2H$_2$O (**1**) that Mn(II) is in the +2 oxidation state, the complex is expected to has magnetic moment of 2.18 B.M. with number of unpaired electrons ($n = 1$) corresponding to d^5 configuration, but the experimental value is higher (3.18 B.M.) than expected value. This is probably due to some distortion of the octahedral environment of the manganese(II) ion resulting in a small orbital contribution. The ferric(III) metformin complex has a 2.00 B.M. magnetic moment with configuration d^5 octahedral stereochemistry, hybrid orbital d^{2}sp^3, one unpaired electrons ($n = 1$), spin only equal 1.73 B.M. and expected magnetic moment is 2.25 B.M. The experimental value of μ_{eff} Fe(III) complex is 2.00 B.M. The magnetic moment, configurations, stereochemistry, hybrid orbitals, number of unpaired electrons, spin-only and expected magnetic values of nickel(II) and copper(II) metformin complexes are (0 B.M., d^8, octahedral, d^{2}sp^3, $n = 0$, 0 and 0 B.M.), and (1.23 B.M., d^9, octahedral, sp^{3}d^2, $n = 1$, 1.73 and 1.96 B.M.), respectively. The lower magnetic value of copper(II) metformin complex assigned to that individual magnetic moments are aligned in opposite directions so that they cancel each other to some extent or can be ascribed as due antiferromagnetic coupling. Thus, the value of magnetic moment of a complex would give valuable insights into its constitution and structure. The magnetic susceptibility measurements thus help to predict the possible geometry of the metal complexes. The

magnetic moments (Table 3) of metal complexes are found to be subnormal that may be attributed to the presence of magnetically coupled metal centers in some cases of conjugated systems and may be assigned upon the distorted in the geometric structures [44].

The diffuse solid reflectance spectra of the complexes were recorded (Table 4). The observed spectra of Mn(II), Fe(III), Ni(II), and Cu(II) metformin complexes agreed with the octahedral or distorted geometry. The spectrum of Mn(II) complex shows four medium intensity bands at 16529, 17731, 19531 and 20747 cm^{-1}, which can be assigned to $^6A_{1g} \rightarrow {}^4T_{1g}$(G), $^6A_{1g} \rightarrow {}^4T_{2g}$(G), and $^6A_{1g} \rightarrow {}^4E_g$(G), $^4A_{1g}$(G), respectively, for an Mn(II) ion in an distorted octahedral field [43]. The electronic spectrum of the octahedral Fe(III) complex showed two distinguish bands. These band at 21,097 cm^{-1} may be assigned to the $^6A_1 \rightarrow {}^4A_1$, ^4E(G) transition and the other at 16,129 cm^{-1} to $^6A_1 \rightarrow {}^4T_2$(G) [45]. The reflectance spectrum of the Ni(II) complex showed two identified bands at 14,749 and 22,422 cm^{-1}, assigned to the transitions $^3A_{2g}$(F) $\rightarrow$ $^3T_{1g}$(F) and, $^3A_{2g}$(F) $\rightarrow$ $^3T_{1g}$(P), respectively [44]. The spectrum of the Ni(II) complex suggests an octahedral geometry. The diffuse reflectance spectrum of copper(II) complex is expected to show two allowed transitions (15,038 and 20,284 cm^{-1}), namely $^2B_{1g} \rightarrow {}^2E_g$ and $^2B_{1g} \rightarrow {}^2B_{2g}$. These bands suggested distorted octahedral geometry around Cu(II) [43].

Electron spin resonance

The ESR tool of analysis is useful in discuss the geometry and state of electrons in metal ion of the complexes. In this paper, the ESR spectrum of the Cu(II) complex (Fig. 2) was analyzed and the related parameters are given in Table 5. The solid-state ESR spectra of some of the complexes exhibit axially symmetric g-tensor parameters with $g_\parallel > g_\perp > 2.0023$, indicating that the copper site has a $d_{x^2-y^2}^2$ ground-state characteristic of tetrahedral, square-planar, or octahedral stereochemistry. The $g_\perp > g_\parallel$ for

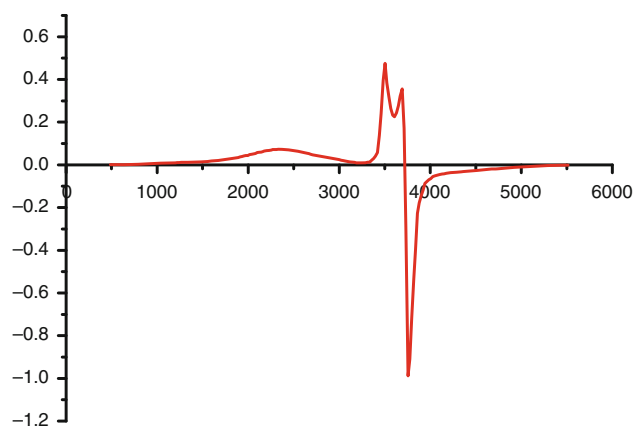**Fig. 2** ESR spectrum of [Cu(MF·HCl)$_2$(Cl)$_2$] (**4**) complex

synthesized Cu(II) metformin complex, [Cu(MF·HCl)$_2$ (Cl)$_2$] (**4**), indicates a distorted octahedral geometry [46]. Figure 2 show splitting, this interpretive according to the interaction between two electrons (copper metal) and metformin HCl ligand because of the location of electrons on different sites.

Proton nuclear magnetic resonance

^{1}H-NMR spectra of metformin HCl free ligand, [Zn(MF· HCl)$_2$](NO$_3$)$_2$·6H$_2$O (**5**), [Cd$_2$(MF·HCl)(Cl)$_4$(H$_2$O)] (**6**), [Mg(MF·HCl)$_2$(Cl)$_2$]·6H$_2$O (**7**), [Ba(MF·HCl)$_2$(Cl)$_2$]·2H$_2$O (**9**), and [Pt(MF)$_4$] (**10**) complexes were recorded in DMSO-d$_6$ taking TMS as internal standards (Table 6). Metformin HCl free ligand (Scheme 1) has assigned as: δ(ppm) 2.920 (6H(A), 2CH$_3$ groups), 3.431 (1H, –NH + 2H, –NH$_2$(C), primary and secondary amine), and (6.845 and 7.251) (2H(B), both =NH imine groups). [Zn(MF· HCl)$_2$](NO$_3$)$_2$·6H$_2$O (**5**) complex: δ(ppm) 2.916 (6H(A), 2CH$_3$ groups), 3.395 (1H, –NH + 2H, –NH$_2$(C), primary and secondary amine), and (6.569 and 7.202) (2H(B), both =NH imine groups). [Cd$_2$(MF·HCl)(Cl)$_4$(H$_2$O)] (**6**) complex: δ(ppm) 2.918 (6H(A), 2CH$_3$ groups), 3.358 (1H, –NH + 2H, –NH$_2$(C), primary and secondary amine), and (6.559 and 7.189) (2H(B), both =NH imine groups). [Mg(MF·HCl)$_2$(Cl)$_2$]·6H$_2$O (**7**) complex: δ(ppm) 2.905 (6H(A), 2CH$_3$ groups), 3.657 (1H, –NH + 2H, –NH$_2$(C), primary and secondary amine), and (6.854 and 7.230) (2H(B), both =NH imine groups). [Ba(MF·HCl)$_2$(Cl)$_2$]· 2H$_2$O (**9**) complex: δ(ppm) 2.912 (6H(A), 2CH$_3$ groups), 3.450 (1H, –NH + 2H, –NH$_2$(C), primary and secondary

Table 6 ^{1}H-NMR spectral data of metformin HCl free ligand, [Zn(MF·HCl)$_2$] (NO$_3$)$_2$·6H$_2$O (**5**), [Cd$_2$(MF·HCl)(Cl)$_4$(H$_2$O)] (**6**), [Mg(MF·HCl)$_2$(Cl)$_2$]·6H$_2$O (**7**), [Ba(MF·HCl)$_2$ (Cl)$_2$]·2H$_2$O (**9**), and [Pt(MF)$_4$] (**10**) complexes

Complexes	Assignments/ppm		
	(6H(A), 2CH$_3$ groups)	(1H, –NH + 2H, –NH$_2$(C), primary and secondary amine)	(2H(B), of both =NH imine groups)
MF·HCl	2.920	3.431	6.845
			7.251
[Zn(MF·HCl)$_2$] (NO$_3$)$_2$·6H$_2$O (**5**)	2.916	3.395	6.569
			7.202
[Cd$_2$(MF·HCl)(Cl)$_4$ (H$_2$O)] (**6**)	2.918	3.358	6.559
			7.189
[Mg(MF·HCl)$_2$ (Cl)$_2$]·6H$_2$O (**7**)	2.905	3.657	6.854
			7.230
[Ba(MF·HCl)$_2$ (Cl)$_2$]·2H$_2$O (**9**)	2.912	3.450	6.852
			7.234
[Pt(MF)$_4$] (**10**)	2.920	3.369	6.767
			7.221
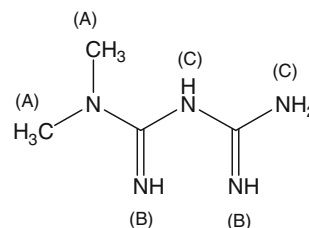
Position of protons	δ-Chemical shift (ppm)
A	2.920
B	6.845
	7.251
C	3.431

Scheme 1 Proton positions and δ-chemical shift (ppm) of free metformin HCl ligand

amine), and (6.852 and 7.234) (2H(B), both =NH imine groups). The ^{1}H-NMR spectrum of Pt(IV) complex has δ(ppm) 2.920 (6H(A), 2CH$_3$ groups), 3.369 (1H, –NH + 2H, –NH$_2$(C), primary and secondary amine), and (6.767 and 7.221) (2H(B), of both =NH imine groups). The previous results can be explain that in the case of cadmium(II) and platinum(IV) complexes, the signal of

Table 5 ESR spectral parameters of the [Cu(MF·HCl)$_2$(Cl)$_2$] (**4**) complex

Complexes	$g_\parallel$	$g_\perp$	g_{av}	$A_\parallel$/cm^{-1}	$A_\perp$/cm^{-1}	A/G	ΔB/G	Assignments
[Cu(MF·HCl)$_2$(Cl)$_2$] (**4**)	1.8253	1.9296	1.8708	94	99	200	110	Distorted octahedral

$A_\parallel$ and $A_\perp$ hyperfine constants; A hyperfine splitting constant; ΔB full width at half max

(1H, –NH + 2H, –NH$_2$(C), primary and secondary amine) was blue shifted in comparison with free metformin HCl ligand, where it can be ascribed to participate in the chelation process. On the other hand, zinc(II), magnesium(II), and barium(II) metformin complexes have decreasing in the intensities of both =NH imine groups. This confirms that both =NH imine groups sharing in the coordination toward central metal atom without proton displacement.

Scanning electron microscopy and X-ray powder diffraction

SEM technique gives a general perception about microstructure, surface morphology, particle size, and chemical composition of respective free metformin HCl ligand, [Fe(MF)$_2$(Cl)$_2$]Cl·4H$_2$O (**2**), [Zn(MF·HCl)$_2$] (NO$_3$)$_2$·6H$_2$O

(**5**), [Mg(MF·HCl)$_2$(Cl)$_2$]·6H$_2$O (**7**), and [Au(MF)$_3$]Cl$_3$ (**11**) complexes. Figure 3a–e designed the SEM photographs of the free ligand and synthesized MF·HCl complexes. The uniformity and similarity between the particles forms of synthesized metformin complexes indicate that the existence of morphological phases of Fe(III), Zn(II), Mg(II), and Au(III) complexes have a homogeneous matrix. A nonspherical oval particles shape (Fig. 3a) is observed in case of the free metformin HCl ligand with the particle size 0.93 μm. A homogeneous phase formation of ferric(III) metformin complex having ice, crack morphologies in the form of a dispersed with particle size 2.0 μm is exhibited in Fig. 3b. The zinc(II) metformin complex has a single phase formation of straight bundle of sticks with particle size 0.67 μm (Fig. 3c). The photo of [Mg(MF·HCl)$_2$(Cl)$_2$]·6H$_2$O (**7**) complex shows a homogeneous solid

Fig. 3 SEM photo of **a** metformin HCl ligand, **b** [Fe(MF)$_2$(Cl)$_2$]Cl·4H$_2$O (**2**), **c** [Zn(MF·HCl)$_2$](NO$_3$)$_2$·6H$_2$O (**5**), **d** [Mg(MF·HCl)$_2$(Cl)$_2$]·6H$_2$O (**7**), and **e** [Au(MF)$_3$]Cl$_3$ (**11**) complexes
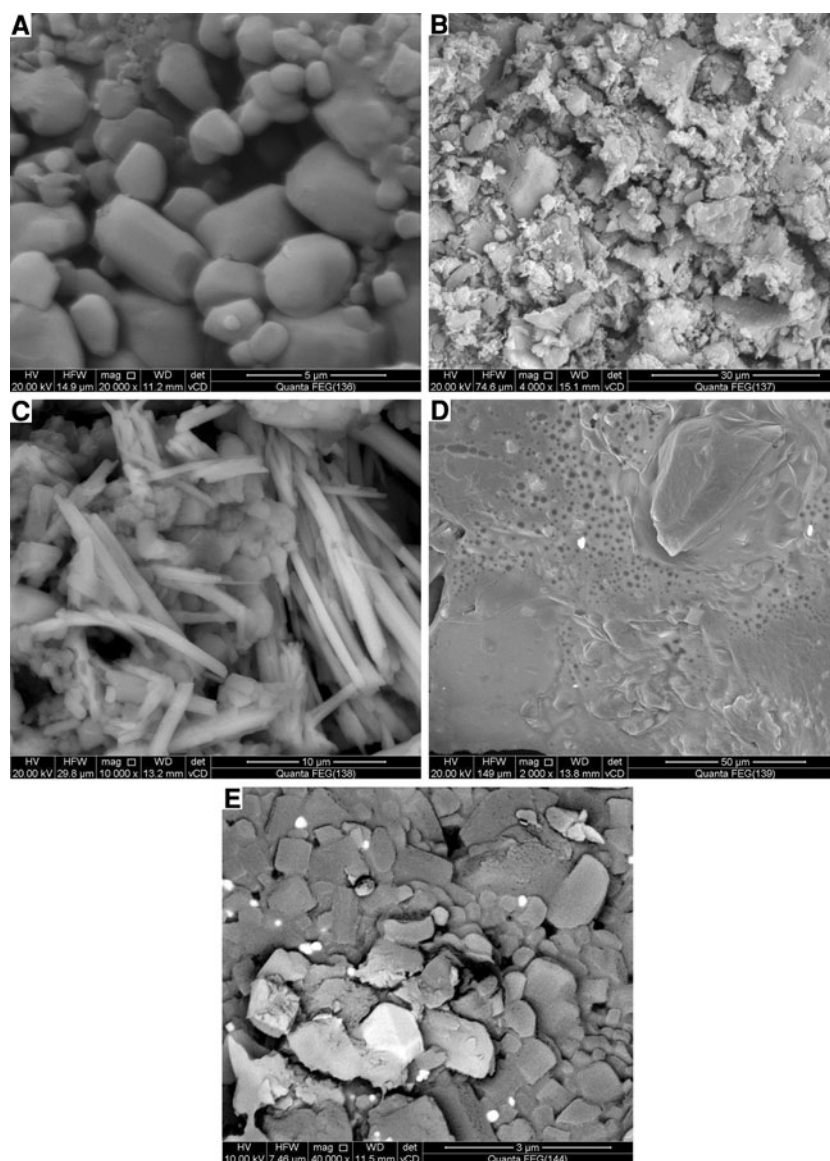
smooth surface, that is hard to designate the size of the particles (Fig. 3d). The grain size distribution of the $[Au(MF)_3]Cl_3$ (**11**) complex is homogeneous (Fig. 3e), where small-to-medium variant particles and the average diameter was found to be 0.40 μm.

XRD patterns in the range of $4° < 2\theta < 80°$ of the metformin HCl free ligand, $[Fe(MF)_2(Cl)_2]Cl·4H_2O$ (**2**), $[Zn(MF·HCl)_2](NO_3)_2·6H_2O$ (**5**), $[Mg(MF·HCl)_2(Cl)_2]·6H_2O$ (**7**), and $[Au(MF)_3]Cl_3$ (**11**) complexes were performed. The diffractograms collected for MF·HCl and their complexes are given in Fig. 4a–e. The detectable diffraction data like angle ($2\theta°$), interplanar spacing (d value, Angstrom), and relative intensity (%) have been summarized in Table 7. The X-ray patterns refer to the crystalline nature for metformin complexes. Comparing the diffractograms of the free metformin HCl ligand with its metal complexes, it can be seen that the clearly variable for the patterns position, which may be attributed to the formation of a new structures (complexation process). The values of 2θ, d value (the volume average of the crystal dimension normal to diffracting plane), full width at half maximum (FWHM) of prominent intensity peak, relative intensity (%)
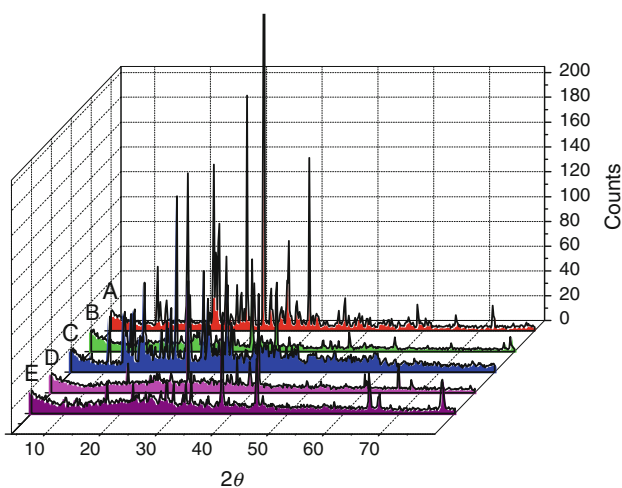
and particle size of complexes were compiled in Table 7. The maximum diffraction patterns of metformin HCl free ligand, $[Fe(MF)_2(Cl)_2]Cl·4H_2O$ (**2**), $[Zn(MF·HCl)_2](NO_3)_2·6H_2O$ (**5**), $[Mg(MF·HCl)_2(Cl)_2]·6H_2O$ (**7**), and $[Au(MF)_3]Cl_3$ (**11**) complexes exhibited at $2\theta/d$-value (Å) = 31.385/2.848, 37.292/2.409, 22.903/3.879, 28.565/3.122, and 38.229/2.352, respectively. The crystallite size could be estimated from XRD patterns by applying FWHM of the characteristic peaks using Deby–Scherrer equation 1 [47].

$$D = K\lambda/\beta\mathrm{Cos}\theta \qquad (1)$$

where D is the particle size of the crystal gain, K is a constant (0.94 for Cμu grid), λ is the X-ray wavelength (1.5406 Å), θ is the Bragg diffraction angle, and β is the integral peak width. The particle size was estimated according to the highest value of intensity compared with the other peaks. These data gave an impression that the particle size was located within nano scale range.

Suggested structures

The metformin hydrochloride (MF·HCl) resulted complexes were characterized using elemental analyses and spectroscopic methods. On the basis of spectral data, ratios of 1:2 (metal:MF) for (Mn(II), Fe(III), Ni(II), Cu(II), Cu(II), Zn(II), Mg(II), Ba(II), and Pd(II)), 2:1 (metal:MF) for (Cd(II) and Sr(II)), 1:3 for Au(III) complex, and 1:4 for Pt(IV) complex. Non electrolytic-to-electrolytic nature of the studied complexes showing the anions is coordinated, uncoordinated or absent to the central metal ion. The magnetic and electronic spectral studies were supported the geometry of for the synthesized complexes as shown in Tables 3 and 4. Based on the spectral data the proposed geometries of the studied complexes are depicted in Fig. 5.

Thermal studies

An analysis of the thermal degradation behavior of metal drug complexes [48–50] is one of the interesting tools to confirm composition and assessment of the role of metal ions. The TG curves of the released metformin hydrochloride free ligands and their **1–10** complexes during static air

Fig. 4 XRD spectra of (*A*) metformin HCl ligand, (*B*) $[Fe(MF)_2(Cl)_2]Cl·4H_2O$ (**2**), (*C*) $[Zn(MF·HCl)_2](NO_3)_2·6H_2O$ (**5**), (*D*) $[Mg(MF·HCl)_2(Cl)_2]·6H_2O$ (**7**), and (*E*) $[Au(MF)_3]Cl_3$ (**11**) complexes

Table 7 XRD spectral data of metformin HCl ligand, $[Fe(MF)_2(Cl)_2]Cl·4H_2O$ (**2**), $[Zn(MF·HCl)_2](NO_3)_2·6H_2O$ (**5**), $[Mg(MF·HCl)_2(Cl)_2]·6H_2O$ (**7**), and $[Au(MF)_3]Cl_3$ (**11**) complexes

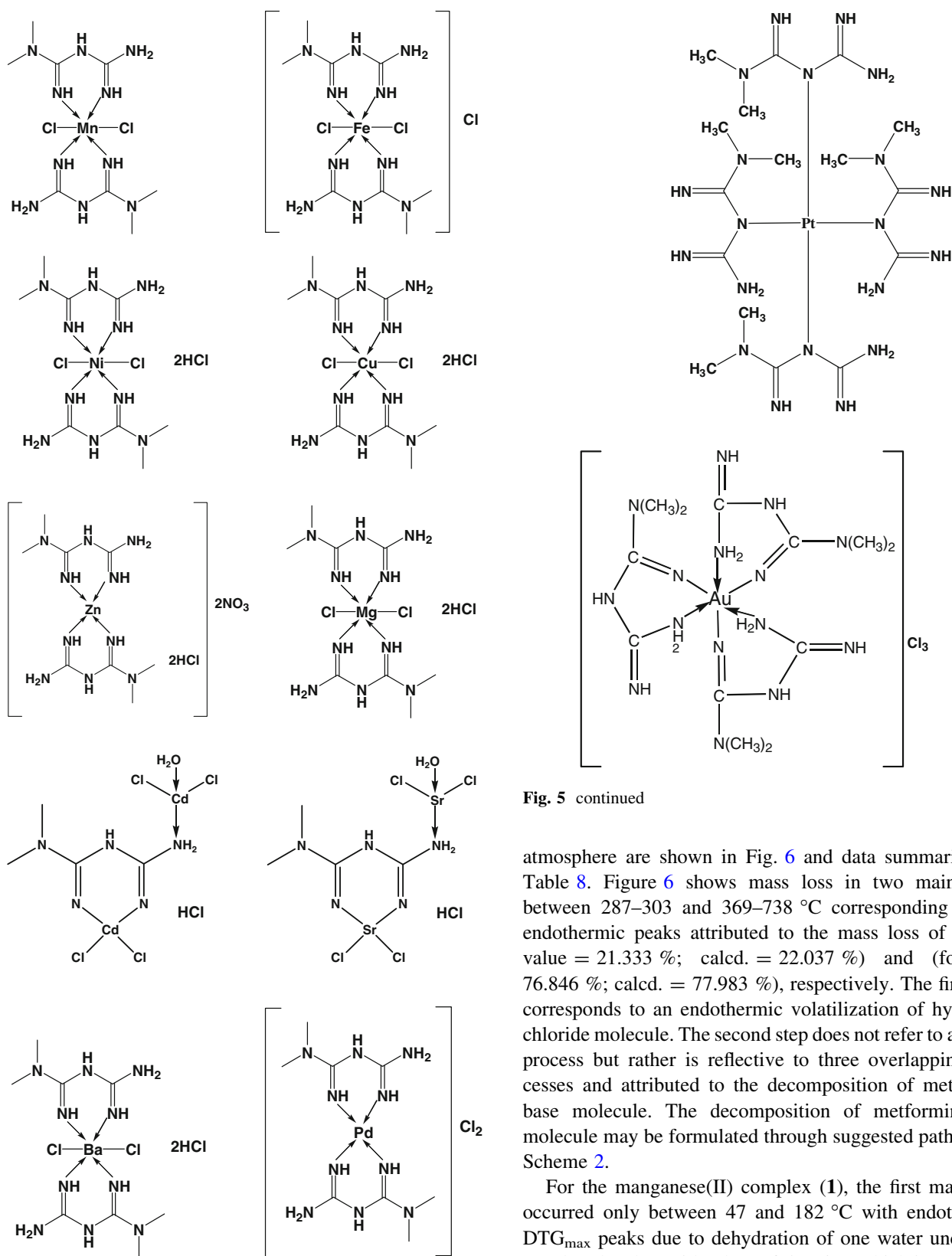| Complexes	$2\theta/°$	d value/Angstrom	Full width at half maximum/FWHM	Relative intensity/%	Particle size/nm
MF·HCl	31.385	2.84797	0.2278	100	7.0
$[Fe(MF)_2(Cl)_2]Cl·4H_2O$ (**2**)	37.292	2.40929	0.2570	100	6.0
$[Zn(MF·HCl)_2](NO_3)_2·6H_2O$ (**5**)	22.903	3.87987	0.1985	100	7.0
$[Mg(MF·HCl)_2(Cl)_2]·6H_2O$ (**7**)	28.565	3.12233	0.1901	100	8.0
$[Au(MF)_3]Cl_3$ (**11**)	38.229	2.35224	0.3322	100	5.0

Fig. 5 Suggested chelating of metformin HCl complexes toward respective metal ions

Fig. 5 continued

atmosphere are shown in Fig. 6 and data summarized in Table 8. Figure 6 shows mass loss in two main steps between 287–303 and 369–738 °C corresponding to the endothermic peaks attributed to the mass loss of (found value = 21.333 %; calcd. = 22.037 %) and (found = 76.846 %; calcd. = 77.983 %), respectively. The first step corresponds to an endothermic volatilization of hydrogen chloride molecule. The second step does not refer to a single process but rather is reflective to three overlapping processes and attributed to the decomposition of metformin base molecule. The decomposition of metformin base molecule may be formulated through suggested pathway in Scheme 2.

For the manganese(II) complex (**1**), the first mass loss occurred only between 47 and 182 °C with endothermic DTG$_{max}$ peaks due to dehydration of one water uncoordinated molecules, with a loss of 5.206 % which is matching with acceptable theoretical calculation 4.284 %. The second water molecule was dehydrated in the second degradation step overlapping with decomposition of two MF molecules
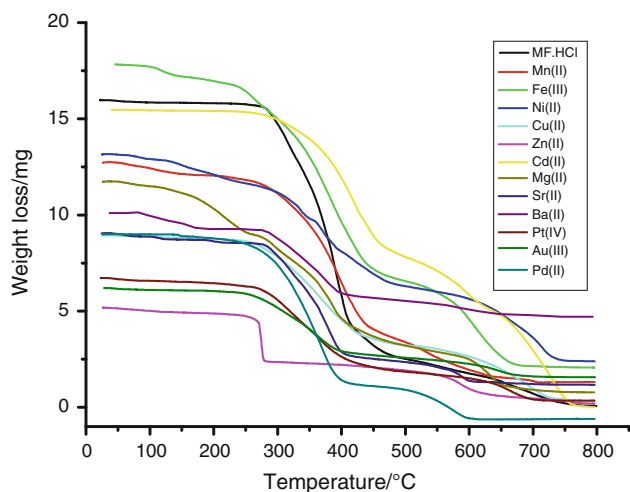
Fig. 6 TG curves of metformin hydrochloride free ligand and their complexes

between 182 and 490 °C, the third decomposition step assigned to the liberation of chlorine molecule of manganese(II) salt with mass loss 17.571 % in agreement with theoretical value 16.898 %. The residual is matched with the formation of manganese oxide.

For the ferric(III) complex (**2**), the first and second mass losses are due to the dehydration stage of four water molecules which occurs between 104 and 310 °C and has totally mass loss of 15.021 % (calcd. = 14.619 %). This stage has a wide range because of the water molecules that interacted with hydrogen of metformin ligand via the formation of hydrogen bonding, which is in agreement with our suggestion. After dehydration steps, the thermal decomposition occurs between 347 and 656 °C in two stages of mass loss. The third and fourth decomposition stages occur with overlapping reactions and correspond to a mass loss of (found = 72.875 %; calcd. = 74.072 %). These mass losses are assigned to the losses of 2MF and 3/2Cl$_2$ molecules. Calculations based on the total mass loss up to 656 °C are in agreement with the formation of iron oxide as a final residual.

Complex (**3**) losses a five uncoordinated water molecules in the 37–252 °C range with three decomposition steps (Fig. 6) (found = 11.699 %, calcd. = 15.817 %). The thermal decomposition of 2MF·HCl and 2HCl occurs in at least three overlapping successive stages as both TG and DTG indicate, the percentage of mass losses (found = 71.045 %, calcd. = 70.693 %). The remaining nickel(II) oxide up to 758 °C was formed.

The decomposition of complex (**4**) comprises in three decomposition stages and starts with decomposition of one MF·HCl and evolved chlorine molecules from 44 to 400 °C range with mass loss (found = 49.284 %, calcd. = 50.811 %). The second metformin hydrochloride molecule starts to decompose at 400–758 °C with mass losses (found = 36.659 %, calcd. = 35.565 %). After the

copper(II) metformin complex decomposed, the copper oxide remain as a final residual product.

Zinc(II) complex (**5**), as it follows from (Fig. 6) and referred in Table 8, the complex is thermally stable up to 789 °C. In the temperature range 132–297 °C, there is one endothermic peak assigned to the loss of six uncoordinated water molecules, 2NO$_3$ and 2HCl species with a mass loss 50.514 % in agreement with theoretical calculation 48.510 %. The release of MF, 2N$_2$H$_4$, and NH$_3$ molecules (found mass loss = 33.896 %, calcd. mass loss = 33.426 %) in temperature range 494–789 °C are observed on TG/DTG curve. The final solid product of thermal decomposition is zinc oxide polluted with carbon atoms.

The complex (**6**) is stable up to 777 °C, then thermal decomposition may be characterized as a two essential decomposition steps in temperature range from 231 to 777 °C. In the first step (231–486 °C), one coordinated water molecule, MF·HCl, and chlorine gas are evaporated (found mass loss = 47.779 %, calcd. mass loss = 46.274 %). In second step mass loss detected in the temperature range 486–777 °C confirmed the release of CdCl$_2$ and cadmium atom (found = 51.788 %, calcd. = 53.726 %). No final solid product of thermal decomposition was recorded.

In case of magnesium(II) metformin complex, the thermal decomposition occurs in four contentious stages with overlapping between third and fourth steps. The first dehydration stage, from 50 to 125 °C is due to the initial decomposition of this complex with mass loss (found = 3.093 %; calcd. = 3.367 %), concerning second decomposition step at 125–260 °C with a mass loss of (found = 20.329 %; calcd. = 20.297 %) was assigned to loss of four water molecules and one hydrogen chloride gas molecule. The total mass loss up to 260 °C (dehydration process in first and second steps) equal to (found = 70.282 %, calcd. = 68.802 %). This percentage is assigned to loss of MF·HCl, MF, and 2HCl molecules. The residual is in agreement with the formation of MgO, as a final residue product.

The [Sr$_2$(MF·HCl)(Cl)$_4$(H$_2$O)] complex (**8**), the thermal decomposition starts at 45 till 210 °C with the release of one mole of hydrogen chloride molecule and in the second step, the release of MF, H$_2$O, SrCl$_2$, Cl$_2$, and Sr atom (started to melt) (found = 81.948 %, calcd. = 75.253 %) are evolved. The final solid product of thermal decomposition is melting strontium oxide with unstable mass loss.
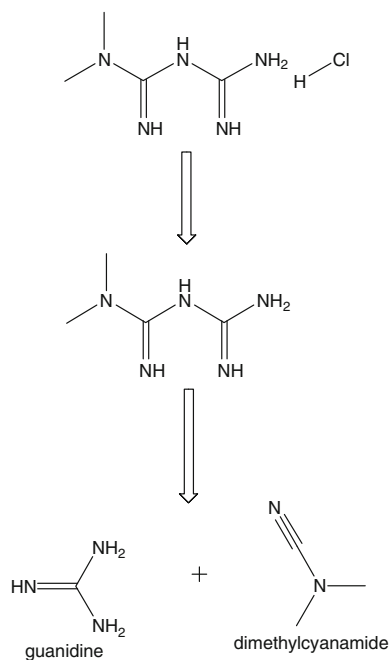
The barium(II) complex (**9**), is stable up to 692 °C, three stages of decomposition take place at different temperature ranges. The first and second steps occurs between 78 and 213 °C with mass loss (found = 8.019 %, calcd. = 6.256 %) due to dehydration of two uncoordinated water molecules, the third decomposition stage between 259 and 692 °C assigned to the decomposition of two mole of MF·HCl. The final decomposition yield discussed as barium(II) chloride contaminated with carbon atoms.

Table 8 Thermogravimetric data of metformin HCl complexes

Complexes	Steps	Temp. range/°C	Decomposed assignments	Weight loss found/calcd./%
MF·HCl	1st	287–303	–HCl	21.333 (22.037)
	2nd	369–408	–CH$_5$N$_3$ (guanidine)	
	3rd	437–462	(CH$_3$)$_2$N-CN	76.846 (77.983)
	4th	666–738	(dimethylcyanamide)	
	Residue			Nil
[Mn(MF)$_2$(Cl)$_2$]·2H$_2$O (**1**)	1st	47–182	–H$_2$O	5.206 (4.284)
	2nd	182–490	–H$_2$O + 2MF	67.398 (65.766)
	3rd	490–731	–Cl$_2$	17.571 (16.898)
	Residue			Manganese oxide
[Fe(MF)$_2$(Cl)$_2$]Cl·4H$_2$O (**2**)	1st	104–123	–H$_2$O	4.078 (3.655)
	2nd	246–310	–3H$_2$O	10.943 (10.964)
	3rd	347–433	–2MF + 3/2Cl$_2$	72.875 (74.072)
	4th	569–656		
	Residue			Iron oxide
[Ni(MF·HCl)$_2$(Cl)$_2$]·6H$_2$O (**3**)	1st	37–109	–H$_2$O	2.164 (3.163)
	2nd	109–184	–2H$_2$O	4.851 (6.327)
	3rd	184–252	–2H$_2$O	4.684 (6.327)
	4th, 5th, 6th	252–758	–2MF·HCl + 2HCl	71.045 (70.693)
	Residue			Nickel oxide
[Cu(MF·HCl)$_2$(Cl)$_2$] (**4**)	1st	44–400	–MF·HCl + Cl$_2$	49.284 (50.811)
	2nd	400–545	–MF·HCl	36.659 (35.565)
	3rd	545–758		
	Residue			Copper oxide
[Zn(MF·HCl)$_2$](NO$_3$)$_2$·6H$_2$O (**5**)	1st	132–297	–6H$_2$O + 2NO$_3$ + 2HCl	50.514 (48.510)
	2nd	494–652	–MF + 2N$_2$H$_4$ + NH$_3$	33.896 (33.426)
		652–789		
	Residue			Zinc oxide polluted with carbons
[Cd$_2$(MF·HCl)(Cl)$_4$(H$_2$O)] (**6**)	1st	231–486	–H$_2$O + MF·HCl + Cl$_2$	47.779 (46.274)
	2nd	486–638	–CdCl$_2$ + Cd	51.788 (53.726)
	3rd	638–777		
	Residue			Nil
[Mg(MF·HCl)$_2$(Cl)$_2$]·6H$_2$O (**7**)	1st	50–125	–H$_2$O	3.093 (3.367)
	2nd	125–260	4H$_2$O + HCl	20.329 (20.297)
	3rd	260–495	–MF·HCl + MF + 2HCl	70.282 (68.802)
	4th	495–767		
	Residue			Magnesium oxide
[Sr$_2$(MF·HCl)(Cl)$_4$(H$_2$O)] (**8**)	1st	45–210	–HCl	5.605 (7.289)
	2nd	261–607	MF + H$_2$O + SrCl$_2$ + Cl$_2$ + Sr metal(melt)	81.948 (75.253)
	Residue			Strontium oxide (still melting)
[Ba(MF·HCl)$_2$(Cl)$_2$]·2H$_2$O (**9**)	1st	78–125	–H$_2$O	3.291 (3.128)
	2nd	125–213	–H$_2$O	4.728 (3.128)
	3rd	259–692	–2MF·HCl (decomposed)	45.256 (47.088)
	Residue			BaCl$_2$ + residual carbons
[Pt(MF)$_4$] (**10**)	1st	22–104	–4MF	69.328 (70.896)
	2nd	237–347		
	3rd	347–496		
	Residue			PtC

Table 8 continued

Complexes	Steps	Temp. range/°C	Decomposed assignments	Weight loss found/calcd./%
[Au(MF)$_3$]Cl$_3$ (**11**)	1st	202–431 ⎫	–3MF + 3/2Cl$_2$	72.438 (71.488)
	2nd	431–741 ⎭		
	Residue			Au metal
[Pd(MF)$_2$]Cl$_2$ (**12**)	1st	122–156 ⎫	–2MF + PdCl$_2$	100 (100)
	2nd	156–459 ⎬	(decomposed)	
	3rd	459–642 ⎭		
	Residue			Nil

Scheme 2 Proposed degradation model of metformin hydrochloride ligand

The platinum(IV) complex (**10**) decomposition of 4MF in a three overlapping steps in the temperature range 22–496 °C. The observed mass loss of 69.328 % is in good agreement with the theoretical value 70.892 %. The residue at this stage has platinum carbide residual product.
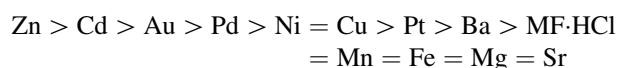
The gold(III) metformin complex (**11**) shows two endothermic stages of decomposition as is evident from the DTG maxima peaks in 202–741 °C range. Both stages of decomposition with a mass loss of (found = 72.438 %, calcd. = 71.488 %) may be attributed to the loss of the 3MF and 3/2Cl$_2$ molecules. On further heating, the gold metal is formed as a final residual product. For the palladium(II) complex (**12**), the simultaneous TG curve in air atmosphere shown in Fig. 6. The thermal decomposition of the anhydrous complex occurs in three overlapping steps cannot be defined between 122 and 642 °C, corresponding to three endothermic peaks with mass loss 100 % assigned to liberate of 2MF and PdCl$_2$ (melt and decomposed).
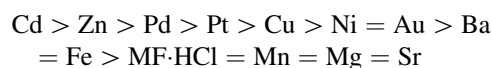
Antimicrobial and anti-cancer studies

In vitro biocidal activities results of both metformin hydrochloride free ligand and their metal complexes clearly show that the compounds have both antibacterial and antifungal potency against the tested organisms (Table 9, and illustrated in Fig. 7). By comparison between the biological evaluation of metformin HCl complexes with the standards Tetracycline as (antibacterial agent) and amphotericin B as (antifungal agent), the results items of highest-to-lowest effective can be summarized as follows:
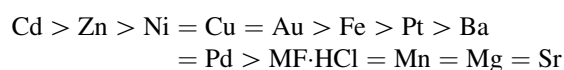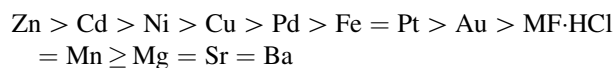
(i) *B. subtilis*

Zn > Cd > Au > Pd > Ni = Cu > Pt > Ba > MF·HCl = Mn = Fe = Mg = Sr

(ii) *E. coli*

Cd > Zn > Pd > Pt > Cu > Ni = Au > Ba = Fe > MF·HCl = Mn = Mg = Sr

(iii) *P. aeruginosa*

Cd > Zn > Ni = Cu = Au > Fe > Pt > Ba = Pd > MF·HCl = Mn = Mg = Sr

(iv) *S. aureus*

Zn > Cd > Ni > Cu > Pd > Fe = Pt > Au > MF·HCl = Mn ≥ Mg = Sr = Ba

(v) *A. flavus*

Cd > Pt > Pd > Au > MF·HCl = Mn = Fe = Ni = Cu = Zn = Mg = Sr = Ba

(vi) *C. albicans*

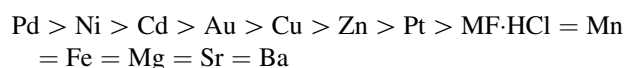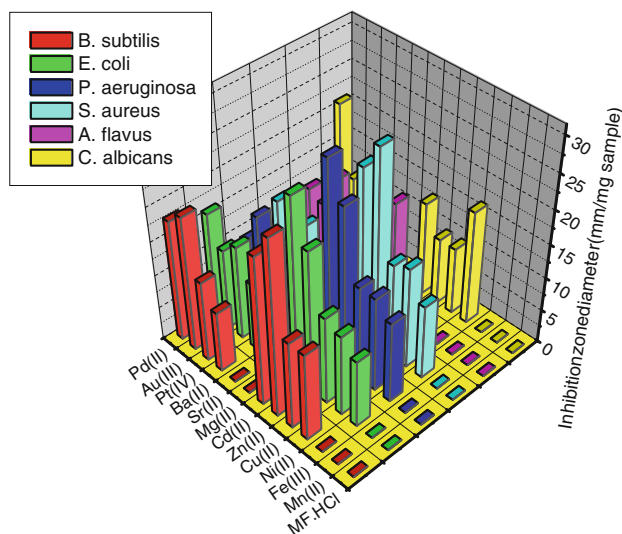Pd > Ni > Cd > Au > Cu > Zn > Pt > MF·HCl = Mn = Fe = Mg = Sr = Ba

Table 9 The inhibition zone diameter (mm/mg sample) of metformin complexes against some kind of bacteria and fungi

Sample	Inhibition zone diameter (mm/mg sample)					
	B. subtilis (G$^+$)	*E. coli* (G$^-$)	*P. aeruginosa* (G$^-$)	*S. aureus* (G$^+$)	*A. flavus/* fungus	*Candida albicans/* fungus
Control: DMSO	0	0	0	0	0	0
Standard						
Tetracycline antibacterial agent	34	32	34	30	–	–
Amphotericin B antifungal agent	–	–	–	–	18	19
MF·HCl	0	0	0	0	0	0
Mn(II)	0	0	0	0	0	0
Fe(III)	0	10	12	11	0	0
Ni(II)	13	12	14	15	0	17
Cu(II)	13	13	14	14	0	10
Zn(II)	26	21	24	29	0	10
Cd(II)	22	27	29	25	17	14
Mg(II)	0	0	0	0	0	0
Sr(II)	0	0	0	0	0	0
Ba(II)	9	10	9	0	0	0
Pt(IV)	12	14	10	11	15	8
Au(III)	20	12	14	9	10	11
Pd(II)	18	16	9	12	11	21

– G: Gram reaction

Fig. 7 Inhabitation zone diameter of metformin complexes toward some kind of bacteria and fungi

The increase in the lipophilicity behavior of these complexes seems to be responsible for their enhanced potent antibacterial activity. Accordingly, these complexes deactivate various cellular enzymes, which play a vital role in various metabolic pathways of these microorganisms. It has also been proposed that the ultimate action of the toxicant is the denaturation of one or more proteins of the cell, which as a result, impairs normal cellular processes.

References

1. Stepensky D, Friedman M, Srour W, Raz I, Hoffman A. Pre-clinical evaluation of pharmacokinetic–pharmacodynamic rationale for oral CR metformin formulation. J Control Release. 2001;71:107–15.
2. Physicians. New Jersey: Desk Reference, Inc., Medical Economics Company; 2003, vol. 57.
3. The Merck Index. Published on CD by Chapman & Hall CRC. Whitehouse Station: Merck & Co Inc, Monograph No. 6001; 1999.
4. Damico C. Nursing, drug handbook. 22nd ed. Springhouse: Springhouse Publishers; 2002. p. 779.
5. Bailey CJ. The anti-hyperglycemic action of metformin. In: Krans HMJ, editor. Diabetes and metformin: a research and clinical update. Royal Society of Medicine international congress and symposium series, No. 79. London: Royal Society of Medicine; 1985. p. 17–26.
6. Hermann LS. Metformin: a review of its pharmacological properties and therapeutic use. Diabetes Metab. 1979;5(3):233–45.
7. Hermann LS. Metabolic effect of metformin in relation to clinical effects and side-effects. In: van der Kuy A, Hulst SGT, editors. Biguanide therapy today. Royal Society of Medicine international congress and symposium series, No. 48. London: Academic Press/Grune & Stratton; 1981. p. 17–48.

8. Lu LP, Zhang HM, Feng SS, Zhu ML. Two *N,N*-dimethylbi-guanidium salts displaying double hydrogen bonds to the counter-ions. Acta Crystallogr C. 2004;60(10):o740–3.

9. Dolzhenko AV, Kotegov VP, Godina AT, Syropiatov BI, Kolotova NV, Koz'minykh VO. Hypoglycemic activity of substituted amides and hydrazides of succinic acid. Eksp Klin Farmakol. 2003;66(3):36–8.

10. Tucker GT, Casey C, Phillips PJ, Conner H, Ward JD, Woods HF. Metformin kinetics in healthy subjects and in patients with diabetes mellitus. Br J Clin Pharmacol. 1981;12(2):235–46.

11. Pentikainen PJ, Neovonen PJ, Pentilla A. Pharmacokinetics of metformin after intravenous and oral administration to man. Eur J Clin Pharm. 1979;16(3):195–202.

12. Sirtori CR, Franceschni G, Gallikienle M. Disposition of met-formin (*N,N*-dimethylbiguanide) in man. Clin Pharm Ther. 1978; 24(6):683–93.

13. Melander A, Wahlin-Boll E. Clinical pharmacology of oral antidiabetic agents. Acta Endocrinol Suppl. 1984;105(262): 119–23.

14. Vigneri R, Goldfine ID. Role of metformin in treatment of dia-betes mellitus. Diabetes Care. 1987;10(1):118–22.

15. Klepser TB, Kelly MW. Metformin hydrochloride: an antihy-perglycemic agent. Am J Health Syst Pharm. 1997;54:893–903.

16. Bentefrit F, Morgant G, Viossat B, Leonce S, Guilbaud N, Pierre A, Atassi G, Dung NH. Synthesis and antitumor activity of the metformin platinum (IV) complex. Crystal structure of the tet-rachloro(metformin)platinum (IV) dimethylsulfoxide solvate. J Inorg Biochem. 1997;68(1):53–9.

17. Viossat B, Tomas A, Nguyen-Huy D. L'hydrogénocarbonate de Bis(*N,N*-diméthylbiguanide) Cuivre(II), [Cu(C$_4$H$_{11}$N$_5$)$_2$]2HCO$_3$. Acta Crystallogr. 1995;C51:213–5.

18. Lemoine P, Chiatdmi M, Bissery V, Tomas A, Viosssat B. Les composés de la metformine avec les ions Co^{II}. Cu^{II} et Ni^{II}. Acta Crystallogr. 1996;C52(6):1430–6.

19. Zhu M, Lu L, Yang P, Jin X. Bis(1,1-dimethylbiguanido)cop-per(II) octahydrate. Acta Crystallogr. 2002;E58:m217–9.

20. Refat MS, El-Metwaly NM. Legitional behavior of 5,5-diethyl-barbituric acid sodium salt (HL) towards Mg, Ca, Sr, Ba(II), spectral, thermal and biological studies. J Mol Struct. 2011; 988(1–3):111–8.

21. Refat MS, Mohamed SF. Spectroscopic, thermal and antitumor investigations of sulfasalazine drug in situ complexation with alkaline earth metal ions. Spectrochim Acta A. 2011;82:108–17.

22. Refat MS. Synthesis, characterization, thermal and antimicrobial studies of diabetic drug models: complexes of vanadyl(II) sulfate with ascorbic acid (vitamin C), riboflavin (vitamin B2) and nic-otinamide (vitamin B3). J Mol Struct. 2010;969:163–71.

23. Refat MS, El-Shazly SA. Identification of a new anti-diabetic agent by combining VOSO$_4$ and vitamin E in a single molecule: studies on its spectral, thermal and pharmacological properties. Eur J Med Chem. 2010;45(7):3070–9.

24. Bauer AW, Kirby WM, Sherris C, Turck M. Antibiotic suscep-tibility testing by a standardized single disk method. Am J Clin Pathol. 1966;45(4):493–6.

25. Pfaller MA, Burmeister L, Bartlett MA, Rinaldi MG. Multicenter evaluation of four methods of yeast inoculum preparation. J Clin Microbiol. 1988;26(8):1437–41.

26. National Committee for Clinical Laboratory Standards. Perfor-mance vol. antimicrobial susceptibility of Flavobacteria; 1997.

27. National Committee for Clinical Laboratory Standards. Methods for dilution antimicrobial susceptibility tests for bacteria that grow aerobically. Approved Standard M7-A3. Villanova: National Committee for Clinical Laboratory Standards; 1993.

28. National Committee for Clinical Laboratory Standards. Refer-ence method for broth dilution antifungal susceptibility testing of conidium-forming filamentous fungi: proposed standard M38-A. Wayne: NCCLS; 2002.

29. National Committee for Clinical Laboratory Standards. Methods for antifungal disk diffusion susceptibility testing of yeast: pro-posed guideline M44-P. Wayne: NCCLS; 2003.

30. Liebowitz LD, Ashbee HR, Evans EGV, Chong Y, Mallatova N, Zaidi M, Gibbs D. Global Antifungal Surveillance Group: a two years global evaluation of the susceptibility of *Candida* species to fluconazole by disk diffusion. Diagn Microbiol Infect Dis. 2001; 4:27–33.

31. Matar MJ, Ostrosky-Zeichner L, Paetznick VL, Rodriguez JR, Chen E, Rex JH. Correlation between E-test, disk diffusion and microdilution methods for antifungal susceptibility testing of fluconazole and voriconazole. Antimicrob Agents Chemother. 2003;47:1647–51.

32. Geary WJ. The use of conductivity measurements in organic solvents for the characterisation of coordination compounds. Coord Chem Rev. 1971;7(1):81–122.

33. Refat MS. Synthesis and characterization of norfloxacin-transi-tion metal complexes (group 11, IB): spectroscopic, thermal, kinetic measurements and biological activity. Spectrochim Acta A. 2007;68(5):1393–405.

34. Bellamy LJ. The infrared spectra of complex molecules. 3rd ed. London: Chapman and Hall; 1975.

35. Socrates G. Infrared characteristic group frequencies. 1st ed. New York: Wiley; 1980.

36. Shanmugam R, Sathyanarayana DN. Raman and polarized infrared spectra of pyridine-2-thione. Spectrochim Acta A. 1984;40(8):757–61.

37. Sharma A, Gupta VP, Virdi A. RHF and DFT based study of the structure, thermodynamic properties and electronic spectra of methacryloyl halides. Indian J Pure Appl Phys. 2004;42(4): 251–7.

38. Dalton F, Hill RD, Meakins GD. The infrared spectra of deute-rium compounds. Part I. The C–H stretching bands of OMe and NMe groups. J Chem Soc. 1960;590:2927–9.

39. Nakamoto K. Infrared and Raman spectra of inorganic and coordination compound. New York: Wiley; 1978.

40. Singh HL, Varshney AK. Synthetic, structural, and biochemical studies of organotin(IV) with Schiff bases having nitrogen and sulphur donor ligands. Bioinorg Chem Appl. 2006. doi:10.1155/BCA/2006/23245.

41. Ozturk OF, Sekerci M, Ozdemir E. Synthesis of 5,6-*O*-cyclo-hexylidene-1-amino-3-azahexane and its Co(II), Ni(II), Cu(II) complexes. Russ J Coord Chem. 2005;31(9):687–90.

42. Ozturk OF, Sekerci M, Ozdemir E. Preparation of complexes of 1-amino-6,7-*O*-cyclohexylidene-4-azaheptane with transition metal acetates. Russ J Gen Chem. 2006;76:33–6.

43. Allan JR, Baird ND, Kassyk AL. Some first row transition metal complexes of nicotinamide and nicotinic acid. J Therm Anal. 1979;16(1):79–90.

44. Lever ABP. The electronic spectra of tetragonal metal complexes analysis and significance. Coord Chem Rev. 1968;3(2):119–40.

45. Bailar JC, Emeleus H, Nyholm JR, Dickenson AF. Comprehensive inorganic chemistry, vol. III. Oxford: Pergamon Press; 1975. p. 517.

46. Cozar O, David L, Chis V, Damian G, Todica M, Agut C. IR and ESR studies on some dimeric copper(II) complexes. J Mol Struct. 2001;563–564:371–5.

47. Quan CX, Bin LH, Bang GG. Preparation of nanometer crystal-line TiO$_2$ with high photo-catalytic activity by pyrolysis of titanyl organic compounds and photo-catalytic mechanism. Mater Chem Phys. 2005;91(2–3):317–24.

48. Kobelnik M, Cassimiro DL, de Almeida AE, Ribeiro CA, Crespi MS. Study of the thermal behavior of Al(III) and In(III)-diclofenac complexes in solid state. J Therm Anal Calorim. 2011;105:415–9.

49. Uivarosi V, Badea M, Olar R, Marinescu D, Nicolescu TO, Nitulescu GM. Thermal degradation behavior of some ruthenium complexes ith fluoroquinolone derivatives as potential antitumor agents. J Therm Anal Calorim. 2011;105:645–50.

50. Badea M, Olar R, Uivarosi V, Marinescu D, Aldea V, Barbuceanu SF, Nitulescu. Thermal behavior of some vanadyl complexes with flavones derivatives as potential insulin-mimetic agents. J Therm Anal Calorim. 2011;105:559–64.